

RESEARCH

Open Access



# A robust estimator of parameters for $\mathcal{G}_l^0$ -modeled SAR imagery based on random weighting method

Cui-Huan Wang<sup>1,2\*</sup> , Xian-Bin Wen<sup>1,2</sup> and Hai-Xia Xu<sup>1,2</sup>

## Abstract

In mono-polarized synthetic aperture radar (SAR) imagery,  $\mathcal{G}_l^0$  distribution often is assumed as the universal model to characterize a large number of targets, which is indexed by three parameters: the number of looks, the scale parameter, and the roughness parameter. The latter is closely related to the number of elementary backscatters in each pixel, and it is the reason why so many researchers focus on it. Although many efforts have been paid on providing many estimates, numerical problems often exist in dependable estimation, such as 'outlier' and small samples and so on. Thus, a robust estimation scheme of two unknown parameters in  $\mathcal{G}_l^0$  distribution based on random weighting method is proposed in this paper where the relationship between moments and parameters are utilized. Experimental results on SAR computational simulations data and real SAR images show that the particular scheme outperforms alternative forms of bias reduction mechanisms, and we can obtain more accurate estimation than that of other state-of-the-art algorithms.

**Keywords:** Synthetic aperture radar (SAR), Random weighting method, Parameter estimation, Robust

## 1 Introduction

In order to interpret synthetic aperture radar (SAR) images, the statistical modeling often be employed. In fact, the multiplicative model using  $\mathcal{G}$  family of distributions often is utilized to describe the speckled data, which is characterized by three parameters: the number of looks, the scale parameter, and the roughness parameter. By this distribution, it is able to describe rough and extremely rough areas, which is better than other distributions [1, 2]. Under the  $\mathcal{G}$  model, regions with different degree of roughness can be characterized by the parameters, thus, the accuracy of the estimation of these parameters becomes very important.

Several kinds of approaches for estimating roughness parameters with different number of looks have been proposed. For example, Gambini et al. gave an analogy estimator based on moments of order 1/2 and 1 [3, 4].

Vasconcellos et al. proposed an analytic change for improving performance with respect to bias and mean-squared error, and the bias in the estimation of the roughness parameter of the  $\mathcal{G}_l^0$  distribution by maximum likelihood (ML) was quantified [5]. In fact, the processing and understanding of SAR image is the problem of small samples, for instance, image filtering where with a few observations within a window a new value is computed. The parameter estimation with small samples is subjected to many problems, mainly including bias, large variance, and sensitivity to deviations from the hypothesized model. On the one hand,  $\mathcal{G}_l^0$  distribution is heavy-tailed distributions. Hence, dealing with SAR data is essentially difficult because samples from the tail of the distribution will have a strong influence on parameter estimation, and bias will be introduced if we decline the weights of them [6]. Therefore, a common issue in all the aforementioned estimation procedures, including ML, and those based on fractional moments and log-cumulants [7] is the need of iterative algorithms for which there is no granted convergence to global solutions. Frery et al. [8] and Pianto and Cribari-Neto [9]

\* Correspondence: wangliu315319@163.com

<sup>1</sup>Key Laboratory of Computer Vision and System, Ministry of Education, Tianjin University of Technology, Tianjin 300384, China

<sup>2</sup>Tianjin Key Laboratory of Intelligence Computing and Novel Software Technology, Tianjin University of Technology, Tianjin 300384, China

proposed techniques to aim at alleviating such issue at the cost of additional computational load.

Random weighting, proposed by Zheng (1987) [10], is an emerging computational method in statistics, and has been used to solve different problems [11]. The random weighting method has following advantages: (1) it is simple in computation; (2) it does not require the previous knowledge on the distribution, and the estimation results are unbiased; (3) the estimation error of the random weighting method is smaller than that of Bootstrap in the case of small samples; (4) it is independent and identically distributed, and robust; (5) statistic determined by the random weighting method has the density function, so it is particularly suitable for the problem described in the density function. This paper is to develop a robust estimation method of combining analogy with random weighting method for the  $\mathcal{G}_I^0$  model, which has the good properties of unbiased, the small mean-

squared error and its ability to resist contamination. Even in small samples and low computational cost, its performance is still very robust.

The paper is organized as follows: Section II presents the random weighting estimation for parameters of  $\mathcal{G}_I^0$  distribution. In Section III, we will present and discuss the main numerical results. Finally, Conclusions and future work are presented in Section IV.

Random weighting estimation for  $\mathcal{G}_I^0$  distribution

1.1 The  $\mathcal{G}_I^0$  model

The multiplicative statistical model is extensively used in SAR image data analyses. Depending on this model, the data are described by a random variable  $X$ , which can be viewed as the product of the independent random variables  $U$  and  $V$ , that is  $X = U \cdot V$ , where  $U$  models the properties of the imaged area (backscatter), and  $V$  models the multiplicative noise (speckle) introduced by

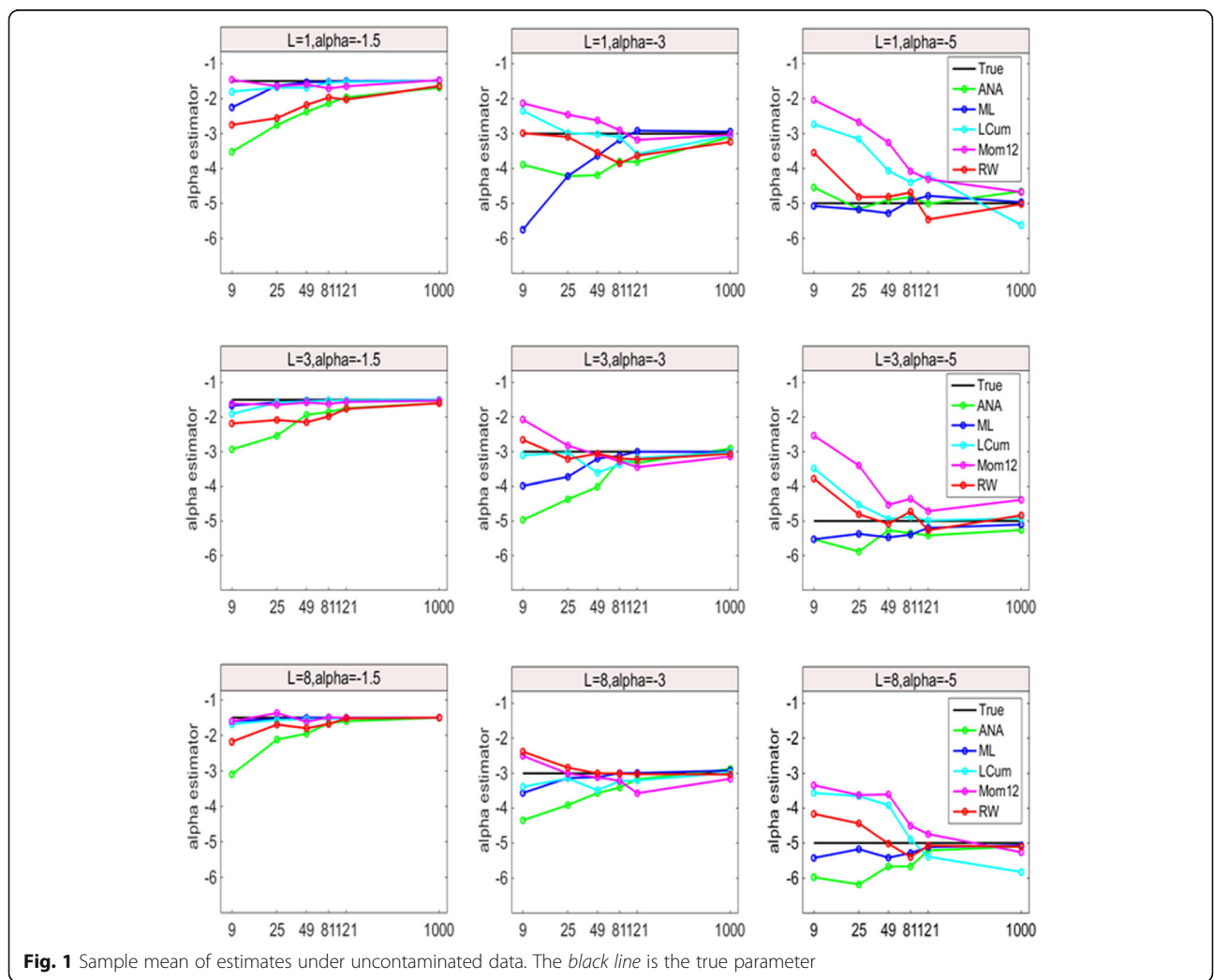


Fig. 1 Sample mean of estimates under uncontaminated data. The black line is the true parameter

the use of coherent illumination, which degrades the image quality. In this manner, speckle noise ( $V$ ) in intensity  $L$ -looks format follows a gamma distribution, denoted by  $\mathcal{G}_I^0(\alpha, \gamma, L)$ , whose probability density is given by

$$f_X(x) = \frac{L^L \Gamma(L-\alpha)}{\gamma^\alpha \Gamma(L) \Gamma(-\alpha)} \frac{x^{L-1}}{(\gamma + Lx)^{L-\alpha}}, \quad x > 0 \quad (1)$$

The backscatter ( $U$ ) exhibits different degrees of homogeneity and can be modeled using the inverse gamma distribution, denoted by  $U \sim \Gamma^{-1}(\alpha, \gamma)$ , whose probability density is

$$\gamma > 0 \quad (2)$$

Then  $X = U \cdot V$  follows a  $\mathcal{G}_I^0(\alpha, \gamma, L)$  distribution [12], whose probability density is

$$f_X(x) = \frac{L^L \Gamma(L-\alpha)}{\gamma^\alpha \Gamma(L) \Gamma(-\alpha)} \frac{x^{L-1}}{(\gamma + Lx)^{L-\alpha}}, \quad x > 0 \quad (3)$$

where  $-\alpha > 0$  is the roughness parameter,  $\gamma > 0$  is the scale parameter and  $L \geq 1$  is the number of looks [1].

The  $r$ -order moments are given by

$$E(X^r) = \left(\frac{\gamma}{L}\right)^r \frac{\Gamma(-\alpha-r)\Gamma(L+r)}{\Gamma(-\alpha)\Gamma(L)} \quad (4)$$

The  $\mathcal{G}_I^0$  distribution is very attractive for modeling data with speckle noise, due to its mathematical tractability and ability to describe information from most types of areas, for given  $\alpha < -1$  and  $L$ . These densities are presented in semi-logarithmic scale, showing that they have heavy (linear) tails with respect to the Gaussian distribution which displays quadratic behavior. It is noticeable that the larger values of  $\alpha$ , the larger the variances have; in fact, the variance is not finite when  $\alpha \geq -1$ .

### 1.2 The random weighting estimator of parameter

Let  $X_1, \dots, X_n$  be independently and identically distributed random variables with distribution  $X \sim \mathcal{G}_I^0(\alpha, \gamma, L)$ ,  $\alpha < -1/2$ ,

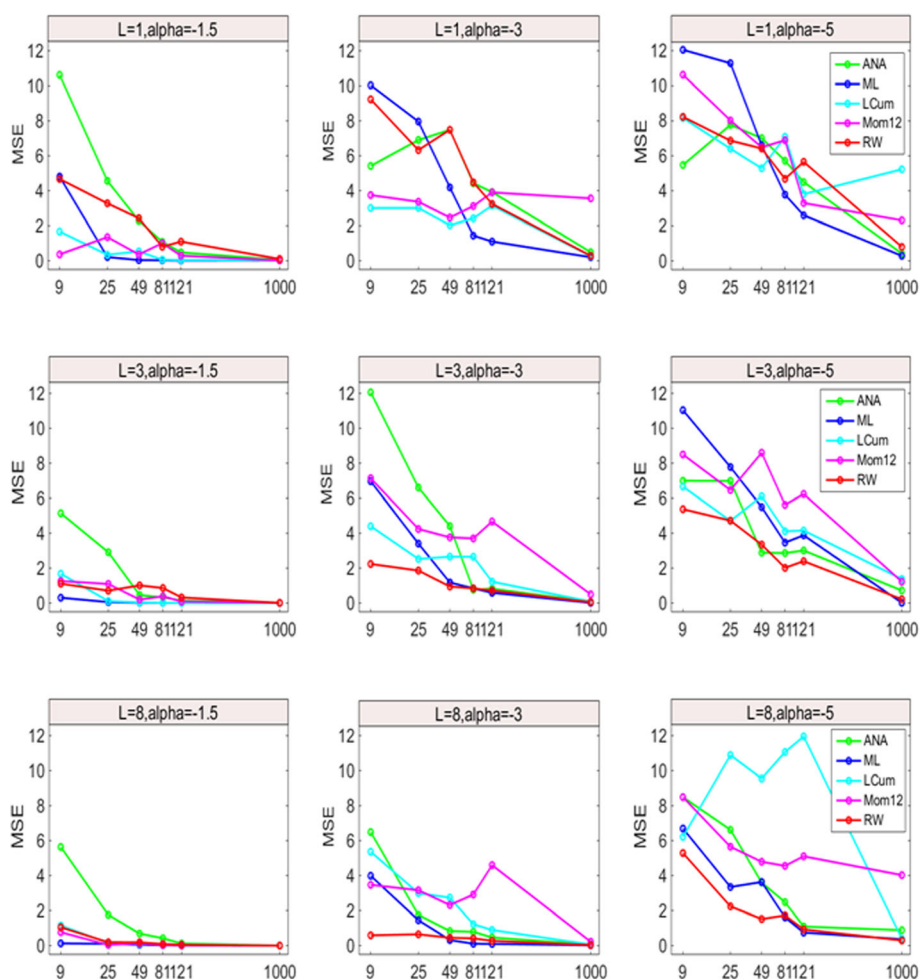
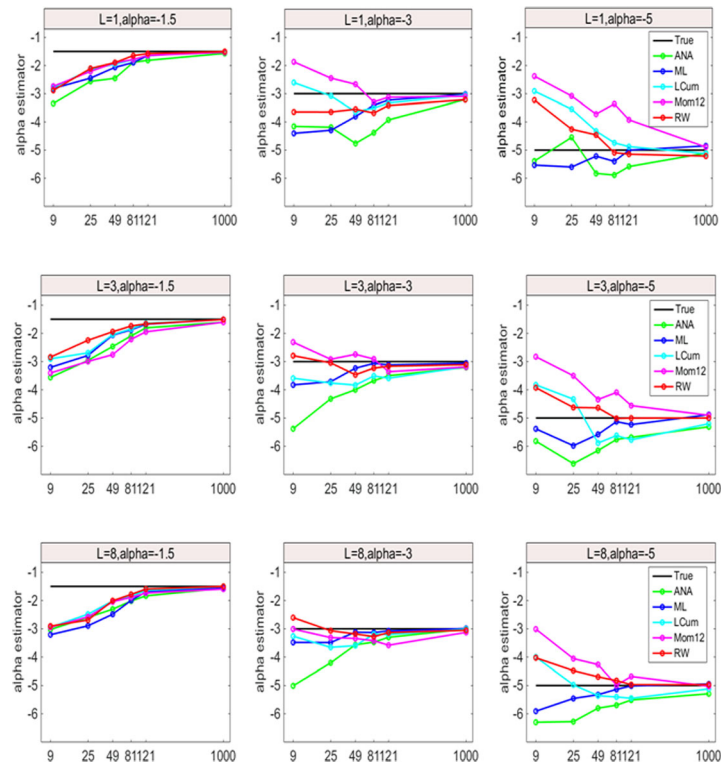
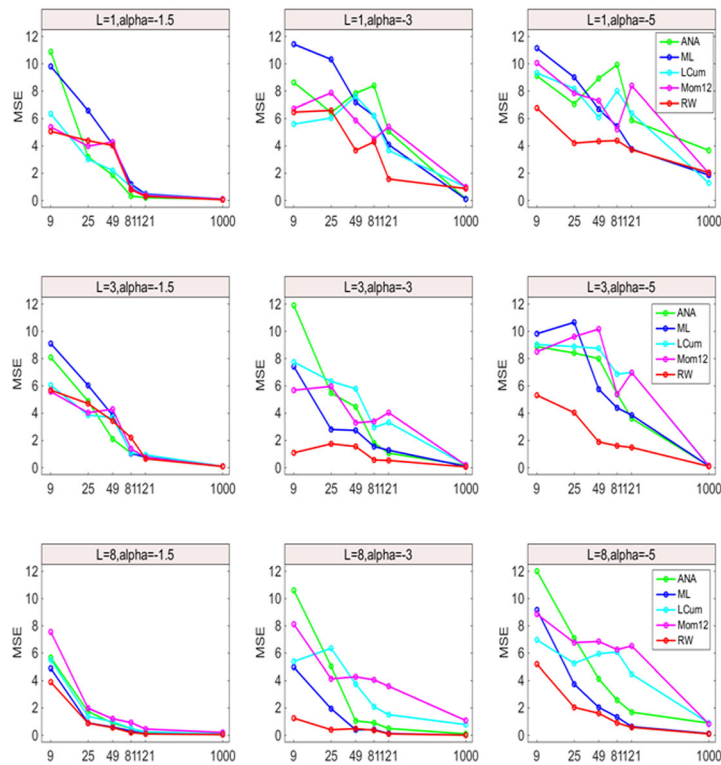


Fig. 2 Sample mean-squared error of estimates under uncontaminated data



**Fig. 3** Sample mean of estimates, case 1 with  $\epsilon = 0.01$  and  $\alpha_2 = -15$



**Fig. 4** Sample mean-squared error of estimates, case 1 with  $\epsilon = 0.01$  and  $\alpha_2 = -15$

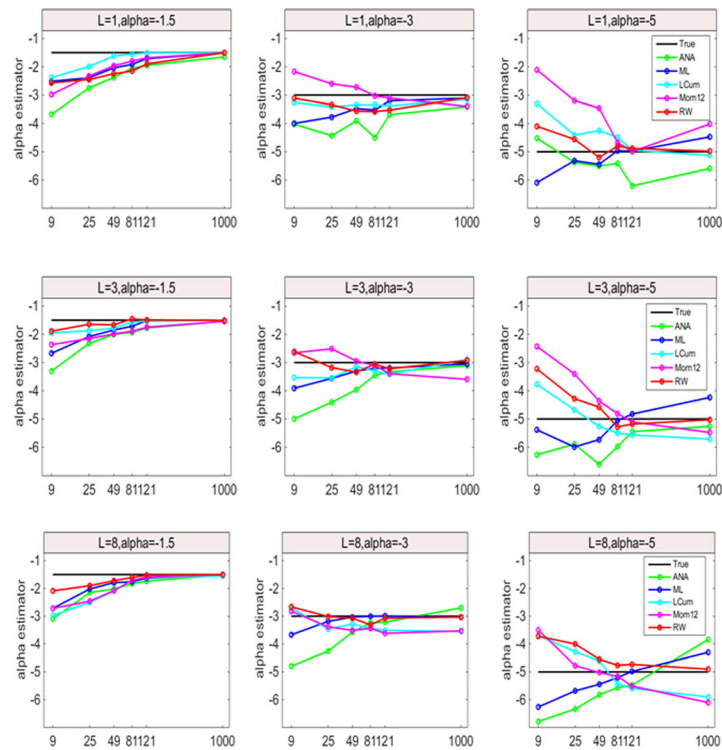


**Fig. 5** Sample mean of estimates, case 2 with  $c = 100$  and  $\epsilon = 0.001$

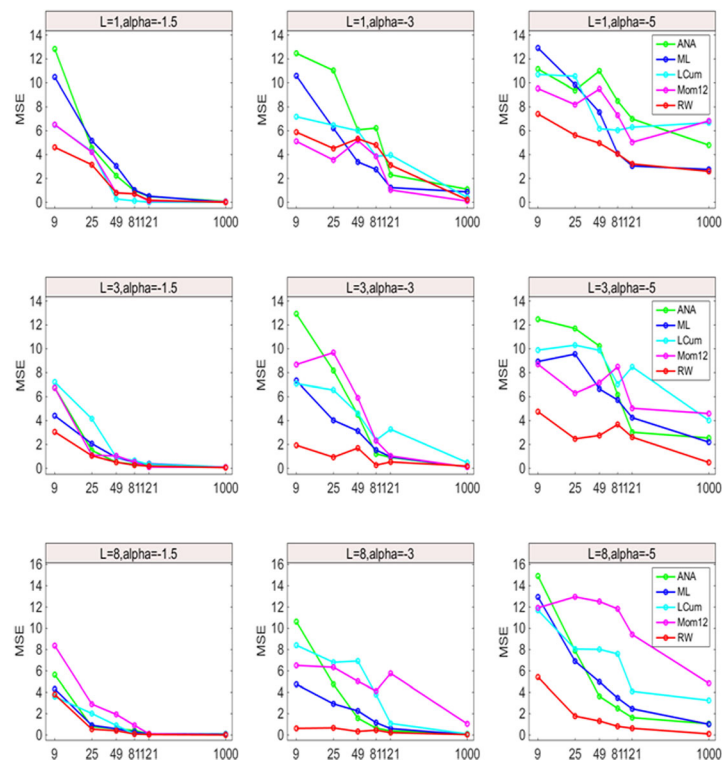


**Fig. 6** Sample mean-squared error of estimates, case 2 with  $c = 100$  and  $\epsilon = 0.001$

$\gamma > 0$  and  $L$  known.  $\bar{X}_n = n^{-1} \sum_{i=1}^n X_i$  and  $\bar{X}_n^r = n^{-1} \sum_{i=1}^n X_i^r$  are the mean of samples and  $r$ th sample moment, respectively, then the random weighting estimation of the  $\bar{X}_n$  and  $\bar{X}_n^r$  can be defined as

$$H_n = \sum_{i=1}^n \xi_i X_i \tag{5}$$

and

$$H_n^r = \sum_{i=1}^n \xi_i X_i^r \tag{6}$$

where  $\xi_1, \dots, \xi_n$  are independent and identically distributed random variable with distribution function of random variable  $\xi_1 = \eta - 2$ , where  $\eta$  is from gamma distribution function  $G(4, 2)$ , i.e., the density function of  $\eta$  is  $\Gamma(4) = \frac{2}{3!}(2x)^3 \exp\{-2x\}I\{x > 0\}$ ,  $I(A)$  is the indicator function of set  $A$ , and  $X_1, \dots, X_n$  and  $\xi_1, \dots, \xi_n$  are mutually independent.

By formula (4), we can know that

$$E(X^{\frac{1}{2}}) = \left(\frac{\gamma}{L}\right)^{\frac{1}{2}} \frac{\Gamma(-\alpha-(1/2))\Gamma(L+(1/2))}{\Gamma(-\alpha)\Gamma(L)}, -\alpha > 1/2 \tag{7}$$

$$E(X) = \left(\frac{\gamma}{L}\right) \frac{\Gamma(-\alpha-1)\Gamma(L+1)}{\Gamma(-\alpha)\Gamma(L)}, -\alpha > 1 \tag{8}$$

Replacing the population moments by their sample counterparts, and the parameters by the corresponding estimators, we arrive at the following system of two equations:

$$\bar{X}_n = \left(\frac{\hat{\gamma}}{L}\right) \frac{\Gamma(-\hat{\alpha}-1)\Gamma(L+1)}{\Gamma(-\hat{\alpha})\Gamma(L)}, -\hat{\alpha} > 1 \tag{9}$$

$$\bar{X}_n^{\frac{1}{2}} = \left(\frac{\hat{\gamma}}{L}\right)^{\frac{1}{2}} \frac{\Gamma(-\hat{\alpha}-(1/2))\Gamma(L+(1/2))}{\Gamma(-\hat{\alpha})\Gamma(L)}, -\hat{\alpha} > 1/2 \tag{10}$$

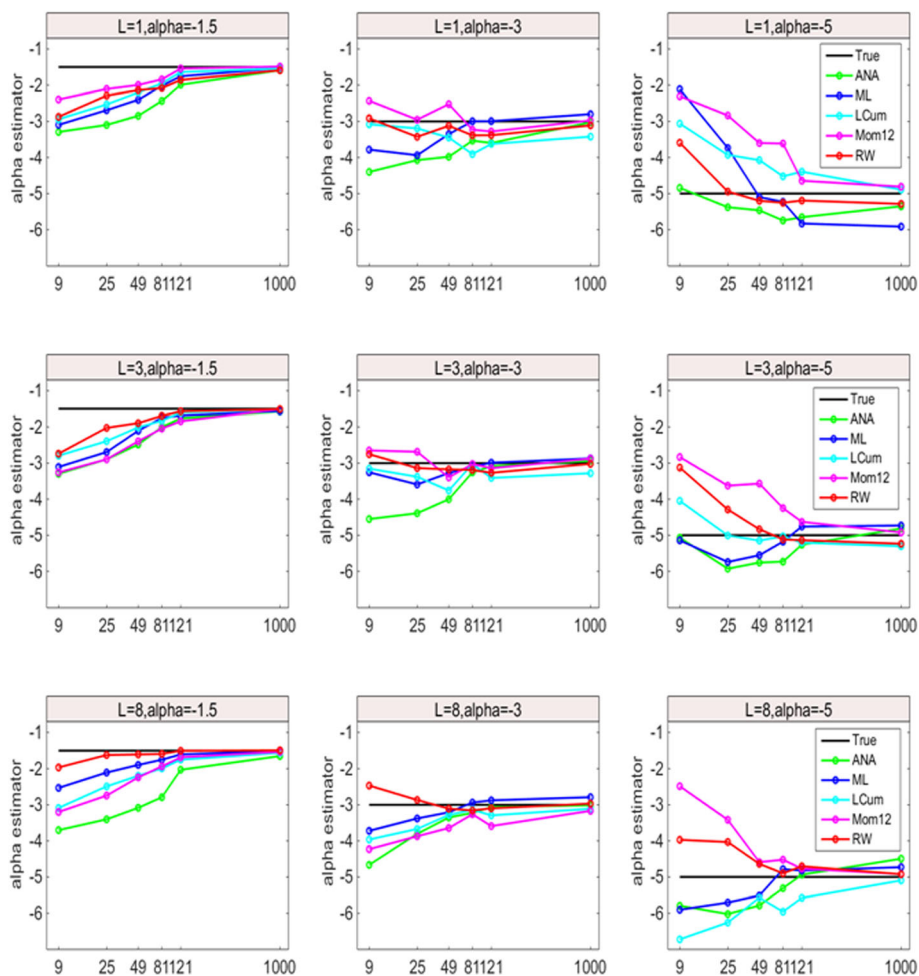


Fig. 7 Sample mean of estimates, case 3 with  $k=2$  and  $\epsilon=0.005$

which lead to the following equation that can be solved numerically in order to obtain an estimator for  $\alpha$ :

$$\frac{\bar{X}_n \Gamma(-\hat{\alpha}) \Gamma(L)L}{\Gamma(-\hat{\alpha}-1) \Gamma(L+1)} = \frac{\left(\bar{X}_n^{\frac{1}{2}}\right)^2 \Gamma^2(-\hat{\alpha}) \Gamma^2(L)L}{\Gamma^2(-\hat{\alpha}-1/2) \Gamma^2(L+(1/2))} \quad (11)$$

By formulas (5) and (6),  $\bar{X}_n, \bar{X}_n^{\frac{1}{2}}$  in (11) is replaced by its random weighting estimation  $H_n, H_n^{\frac{1}{2}}$ , respectively. We have

$$\frac{H_n \Gamma(-\hat{\alpha}) \Gamma(L)L}{\Gamma(-\hat{\alpha}-1) \Gamma(L+1)} = \frac{\left(H_n^{\frac{1}{2}}\right)^2 \Gamma^2(-\hat{\alpha}) \Gamma^2(L)L}{\Gamma^2(-\hat{\alpha}-1/2) \Gamma^2(L+(1/2))} \quad (12)$$

Therefore, the random weighting estimator  $\hat{\alpha}^*$  for  $\alpha$  can be obtained via solving equation (12). By substituting the value of  $\hat{\alpha}^*$  into formula (9), we can obtain random weighting estimator  $\hat{\gamma}^*$ .

## 2 Performance evaluations

In this section, the random weighting estimation of  $\mathcal{G}_I^0$  distribution parameters is comprehensively evaluated on SAR computational simulations data and real SAR images.

### 2.1 Simulations data and analysis

The results of double bounce in SAR system is that a high return value exists in some pixels. The presence of such outliers may provoke big errors in the estimation. Since robustness is the ability to perform well when the data obey the assumed model and to not provide completely useless results when the observations do not exactly follow it, moreover, estimators in SAR signal and image processing are always used in various robustness algorithms, thus, the robustness is of highest importance.

In order to assess the behavior of the proposed estimators, computational simulations have been performed to

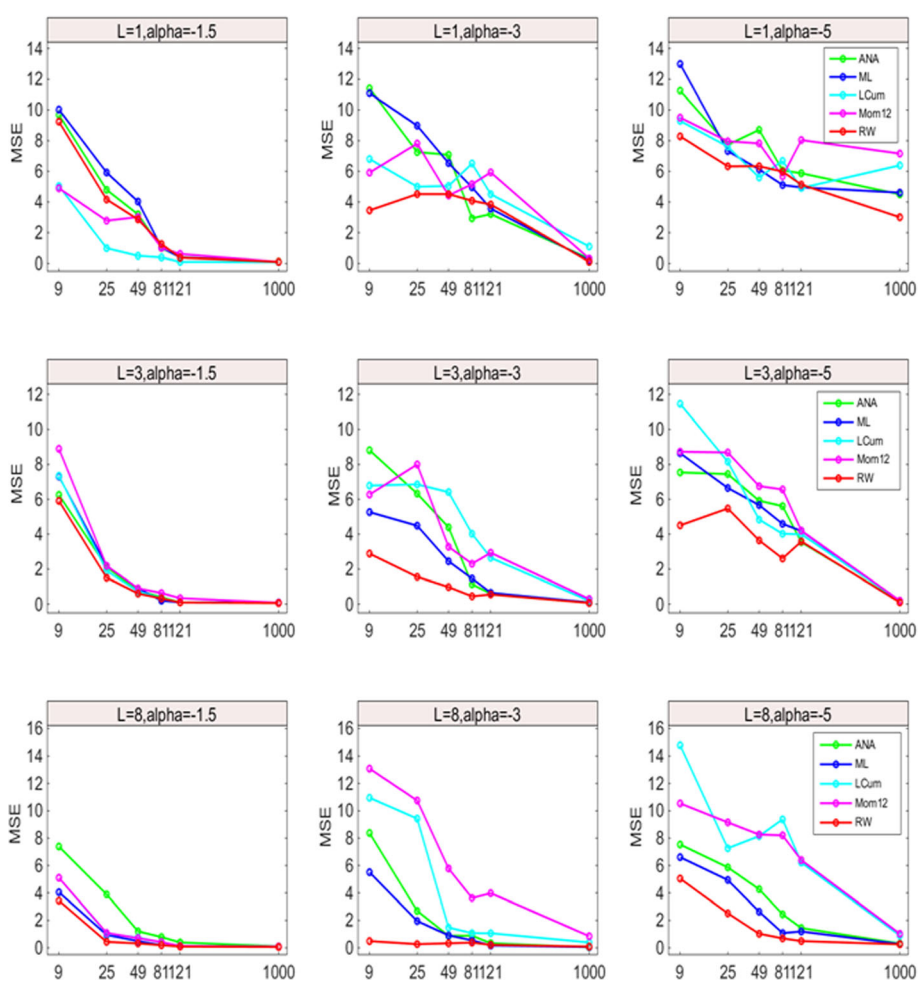
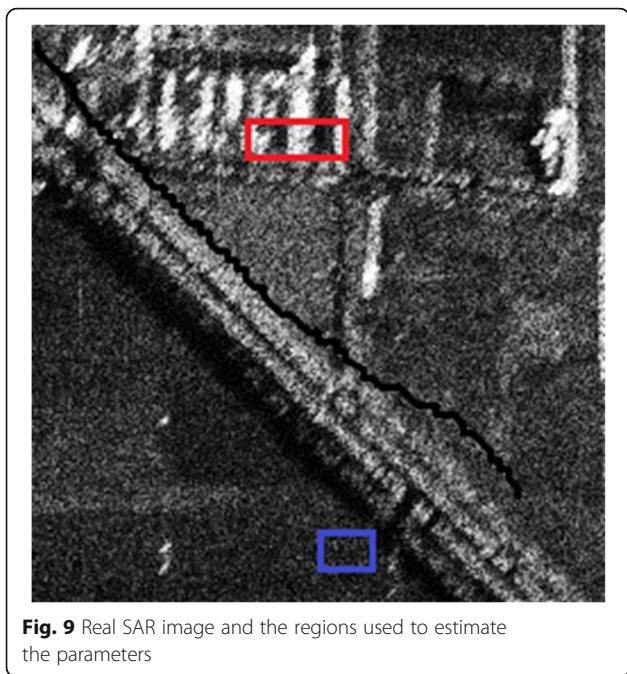


Fig. 8 Sample mean-squared error of estimates, case 3 with  $k=2$  and  $\epsilon=0.005$



**Fig. 9** Real SAR image and the regions used to estimate the parameters

verify random weighting (RW) estimation of parameters  $\alpha$  and  $\gamma$ . Let  $0 < \varepsilon \leq 1, C \in \mathbb{R}_+$ . In these simulation studies, we consider uncontaminated data and three contaminated models, where samples  $\{X_1, \dots, X_n\}$  are identically distributed random variables with one of uncontaminated and three contaminated models. The three patterns of the contamination are defined as follows:

$$\text{Case 1 : } (1-\varepsilon)\mathcal{G}_I^0(\alpha_1, \gamma_1, L) + \varepsilon\mathcal{G}_I^0(\alpha_2, \gamma_2, L)$$

$$\text{Case 2 : } (1-\varepsilon)\mathcal{G}_I^0(\alpha_1, \gamma_1, L) + \varepsilon C$$

$$\text{Case 3 : } (1-\varepsilon)\mathcal{G}_I^0(\alpha_1, \gamma_1, L) + \varepsilon\mathcal{G}_I^0(\alpha_1, 10^k\gamma_1, L)$$

The sample lengths are 9, 25, 49, 81, 121, and 1000, respectively. The parameter  $\alpha$  is evaluated by using different real values such as  $\alpha = \{-1.5, -3, -5\}$ , which are used on behalf of areas with intense and moderate texture. As compared, we simulate the analogy estimator (ANA) [7], maximum likelihood (ML) [8], log-cumulant (LCum) [7] and 1/2-moment (Mom12) [1].

**Table 1** Estimations of the  $\alpha$  parameter using the samples shown in Fig. 9

Color	Size	$\hat{\alpha}_{RW}$	$\hat{\alpha}_{ANA}$	$\hat{\alpha}_{ML}$	$\hat{\alpha}_{LCum}$	$\hat{\alpha}_{Mom12}$
Blue	25	-3.0821	-5.2631	-3.1776	-2.8362	-2.0477
Red	30	-4.2572	-6.9932	-5.6990	-3.0953	-2.0067

**Table 2** Estimations of the  $\gamma$  parameter using the samples shown in Fig. 9

Color	Size	$\hat{\gamma}_{RW}$	$\hat{\gamma}_{ANA}$	$\hat{\gamma}_{ML}$	$\hat{\gamma}_{LCum}$	$\hat{\gamma}_{Mom12}$
Blue	25	2.0821	4.2631	2.1776	2.8362	1.0477
Red	30	3.2572	5.9932	4.6990	2.0953	1.0067

Figures 1, 2, 3, 4, 5, 6, 7, and 8 show a graphical comparison of the mean and variance estimation values for parameter  $\alpha$  after testing 1000 times under uncontaminated data with cases 1, 2, and 3, respectively.

From Figs. 1 and 2, we can observe that only three methods of five estimators are very close to the true value in mean, namely,  $\hat{\alpha}_{ML}$ ,  $\hat{\alpha}_{ANA}$  and  $\hat{\alpha}_{RW}$ , and the farthest estimators from the true value are  $\hat{\alpha}_{LCum}$  and  $\hat{\alpha}_{Mom12}$ , when  $\alpha = -5$ . In most cases, all methods have very similar mean-squared error in the larger sample data, thus, we cannot decide which one is the best. However, our proposed method is better than other four methods especially when  $L = 3$  and  $L = 8$ .

Figures 3 and 4 show the influence of the perturbation in contaminated cases. As expected, it is more obvious. With the increase of the number of sample, the proposed estimation is further away from the contamination, and the mean-squared errors of  $\hat{\alpha}_{RW}$  is smaller than that of  $\hat{\alpha}_{ANA}$ ,  $\hat{\alpha}_{ML}$ ,  $\hat{\alpha}_{LCum}$ ,  $\hat{\alpha}_{Mom12}$  for  $L = 3, 8$ . But all methods do not have clear distinction for  $L = 1$  except that  $\hat{\alpha}_{RW}$  is at least very competitive in the case of  $\alpha = -3$ .

From Figs. 5 and 6, our proposed estimator is approximately close to the true mean value, and its mean-square error is smaller than that of other methods, except for  $L = 1$  and  $\alpha = -3$ .  $\hat{\alpha}_{RW}$  produces the closest estimates to the true value with reduced mean-squared error from Figs. 7 and 8.

### 2.2 Real SAR image and analysis

In order to further prove the performance of our proposed method, practical experiments have been conducted to estimate  $\alpha$  and  $\gamma$  parameters in  $\mathcal{G}_I^0(\alpha, \gamma, L)$ , which is employed to model the real SAR image by random weighting. In these experiments, SAR data from a three-look intensity format SAR image are used. Figure 9 shows the regions used for estimating parameter. Tables 1 and 2 show the results of estimating  $\alpha$  and  $\gamma$  parameters for each rectangular region. Figure 10 shows the histogram and the line of the estimated probability density function by each estimation method for each rectangular region. The Kolmogorov–Smirnov test (KS test) is then performed between  $X$  from the image and  $Y$  for the null hypothesis  $H_0$  “both samples come from the



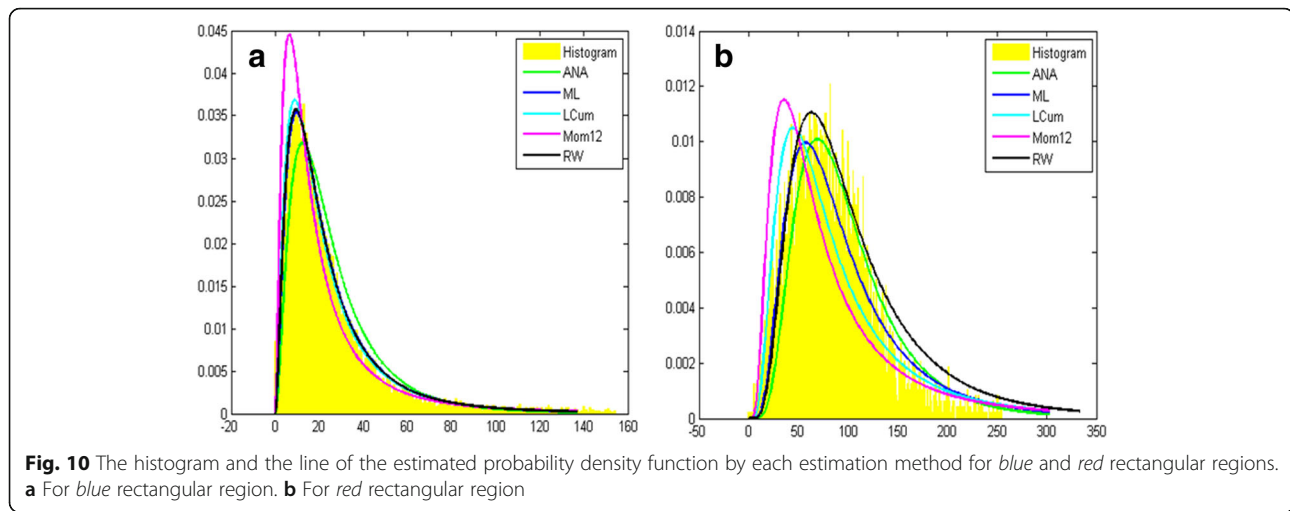


**Fig. 10** The histogram and the line of the estimated probability density function by each estimation method for blue and red rectangular regions. **a** For blue rectangular region. **b** For red rectangular region

same distribution”, and the complementary alternative hypothesis. Table 3 shows the sample  $p$  values. It is observed that the null hypothesis is not rejected with a significance level of 5% in any of the cases. The results justify that the model is adequate for the data, and the performance of our proposed method is better than the others.

### 3 Conclusions

A new estimator for the roughness parameter of the  $c = 100$  distribution based on the random weighing method is proposed. Moreover, three models of contamination inspired in real situations are defined to assess the impact of outliers in the performance of the estimators. By the experiments and analysis under the contamination, we can observe that: (1) do not consider the intensity of the contamination, the bigger the number of looks, the smaller the percentage of no convergence. (2) Under the contamination cases, the convergence with the increase of the level of contamination or with the reduction of  $\alpha$ . In conclusion, our proposed method is much closer to the real mean value, and its mean-squared error is lower than that of other methods in the case of small samples.

**Table 3** Sample  $p$  values of the K–S test with samples from the image in Fig. 9

Color	$p$ value				
	$\hat{a}_{RW}$	$\hat{a}_{ANA}$	$\hat{a}_{ML}$	$\hat{a}_{LCum}$	$\hat{a}_{Mom12}$
Blue	0.5298	0.3722	0.3649	0.2621	0.1541
Red	0.7375	0.5315	0.1969	0.1290	0.1052

### Acknowledgements

This work was supported in part by the National Natural Science Foundation of China (Grant No. 61472278 and 61102125) and the Natural Science Foundation of Tianjin (Grant No. 12JCYBJC10200).

### Authors' contributions

C-HW contributed significantly to the conception of the study and performed the experiments. Moreover, the author analyzed the data and drafted the manuscript; X-BW and H-XX helped perform the analysis with constructive discussions and revised the manuscript; X-BW and H-XX approved the final version. All authors read and approved the final manuscript.

### Authors' information

Cui-Huan Wang received the B.S. degree in Communication Engineering from North College of Beijing University of Chemical Technology, Hebei, China, in 2014.

Currently, she is pursuing her master's degree in School of Computer and Communication Engineering at Tianjin University of Technology, Tianjin, China. Her research interests include synthetic aperture radar (SAR) image processing.

Xian-Bin Wen received the master's degree in Applied Mathematics and the PhD degree in Computer Application Technology both from Northwestern Polytechnical University, Xi'an, China, in 1992 and 2005, respectively.

Currently, he is a Professor with Tianjin University of Technology. His current research interests include remote sensing image understanding, pattern recognition, computer vision, intelligent computer, and statistical signal analysis.

Hai-Xia Xu received the B.S. and PhD degrees in Computer Application Technology from Northwestern Polytechnical University, Xi'an, China.

Currently, she is an associate professor with Tianjin University of Technology. Her research interests include remote sensing image understanding, pattern recognition, and computer vision.

### Competing interests

The authors declare that they have no competing interests.

Received: 9 October 2016 Accepted: 6 February 2017

Published online: 27 February 2017

### References

1. C Frery, HJ M'uller, CCF Yanasse, SJS Sant'Anna, Sant'Anna, A model for extremely heterogeneous clutter. *IEEE Trans Geosci Remote Sens* **35**(3), 648–659 (1997)
2. ME Mejail, I Pabelln, C Universitaria, Approximation of distributions for SAR Images: proposal, evaluation and practical consequences[J]. *Lat. Am. Appl. Res.* **31**(2), 83–92 (2002)

3. J Gambini, M Mejail, J Jacobo-Berlles, AC Frery, Accuracy of edge detection methods with local information in speckled imagery. *Stat. Comput.* **18**, 15–26 (2008)
4. J Gambini, ME Mejail, J Jacobo-Berlles, AC Frery, Feature extraction in speckled imagery using dynamic B-spline deformable contours under the GO model. *Int. J. Remote Sens.* **27**, 5037–5059 (2006)
5. KLP Vasconcellos, AC Frery, LB Silva, Improving estimation in speckled imagery. *Comput Statist* **20**(3), 503–519 (2005)
6. JF Reed III, DB Stark, Hinge estimators of location: robust to asymmetry. *Comput Methods Programs Biomed* **49**, 11–17 (1996)
7. J Gambini, J Cassetti, M Lucini et al., Parameter estimation in SAR imagery using stochastic distances and asymmetric kernels. *IEEE J Sel Top in Appl Earth Obs Remote Sens* **8**(1), 573–576 (2014)
8. AC Frery, F Cribari-Neto, MO Souza, Analysis of minute features in speckled imagery with maximum likelihood estimation. *EURASIP J Adv Signal Process* **16**, 1–16 (2004)
9. DM Pianto, F Cribari-Neto, Dealing with monotone likelihood in a model for speckled data. *Comput Statist Data Anal* **55**, 1394–1409 (2011)
10. Z Zheng, Random weighting method. *Acta Math. Appl. Sin. (Chinese)* **2**, 121–127 (1987)
11. Z Zheng, Random weighting method. *Adv. Math. (China)* **10**, 247–253 (1989)
12. M Mejail, JC Jacobo-Berlles, AC Frery, OH Bustos, Classification of SAR images using a general and tractable multiplicative model. *Int J Remote Sens* **24**(18), 3565–3582 (2003)

**Submit your manuscript to a SpringerOpen<sup>®</sup> journal and benefit from:**

- Convenient online submission
- Rigorous peer review
- Immediate publication on acceptance
- Open access: articles freely available online
- High visibility within the field
- Retaining the copyright to your article

---

Submit your next manuscript at ► [springeropen.com](http://springeropen.com)

---